Proceedings of 20th International Congress on Acoustics, ICA 2010

23-27 August 2010, Sydney, Australia

Modelling of Na D-Line Shape in Sonoluminescence Spectra Based Upon Density Dynamics

Mikhail V. Kazachek (1), Tatyana V. Gordeychuk (1)

(1) V.I. Il'ichev Pacific Oceanological Institute FEBRAS, Vladivostok 690041, Russia

PACS: 78.60.Mg, 33.70, 47.55 dd

ABSTRACT

A new model of the shape of Na D-line in sonoluminescence spectra is presented. The model is based on a hypothesis that a complex structure of the line (the shift, broadening, asymmetry, presence of parent peaks) is formed by the spectra radiated at various densities of the perturbing environment. The interval of the density values during the emission is obtained by fitting of model spectra to experimental data. The best fit is found for the case when a rate of density growth is increased to the moment of full collapse. The estimated density interval when emission occurs is 25-400 Amg for the case of NaCl water solution in argon at 22 kHz. Assuming that the intrabubble temperature is 2000 K, the pressure is about 3000 bar at 400 Amg. It is also proposed that the only origin of narrow parent Na D-line peaks observed in the experimental spectra is "low density" emission. The sonoluminescence spectra of K and Li are studied within the model. It is observed that increasing ultrasound frequency leads to displacing of the boundaries of the density interval to lower values.

INTRODUCTION

Sonoluminescence (SL) arises from acoustic cavitation. "Hot-spot" hypothesis is considered as the most suitable for explanation the SL phenomena when the accumulation of acoustic energy leads to a very high temperature and pressure inside the cavitation bubbles. Within the hypothesis, the observation of alkali-metals lines in SL spectra from salt aqueous solutions testifies that the metals get into emission area, for example, by the mechanism offered in [1], and are undergo the extreme conditions.

We studied the multibubble SL for argon saturated NaCl aqueous solution. The Na D-line exhibits asymmetry towards the red zone in SL spectra [2]. The shift and broadening of the line can be caused by extremely high density of bubble content at the moment of emission. In [3] the line width was used to estimate the density of the perturbing environment at bubble collapse. According to [4], the observation of plasma and high temperatures during single bubble SL in H_2SO_4 means that Stark effect is the dominant factor contributing to the Ar emission line width and shift. In [5] the large Na line width is explained by rapid collisional deactivation of the excited-state atoms (lifetime ~0.05 ps) in dense environment. However the authors did not give any explanation for the line asymmetry.

If to exclude instrumental broadening, other sources of spectral line broadening do not influence the line width [4]. In our case Stark broadening is probable negligible because it is be obviously to expect much less dense plasma during neutral Na emission in MBSL than during argon emission in SBSL [4]. So the main subject of our investigation is the effect of the density of surrounding particles on the Na line shape.

The density changes considerably during the time of emission (Figure 1a). So we believe the complex form of the D-line is a result of imposing of the spectra radiated at various density of perturbing medium. The calculations based on our model show that the shape of an intrabubble density curve changes the profile of the Na D-line. The narrow parent Na doublet peaks, superimposed on the widening band, are observed in some SL spectra [3, 6]. This means that the Na emission occurs at low densities also. According recent experimental paper [7], in laser-created bubble the Na emission and continuum flash are separated in time. In addition the Na emission has a very long duration (10th nanoseconds), while the duration of the SBSL flash is about 150 ps [8]. In theoretical paper [9] was shown that the spectrum of SL is different in different moments of flash. We believe that all of these data give a support for our hypothesis.

Note that the theory and numerical simulation of the bubble dynamics, especially near the «point of return» t = 0 (Figure 1a), needs in experimental confirmations, which are difficult due to the extremeness of process. In our work we investigate the Na line shape from the standpoint of density dynamics during the emission.

EXPERIMENT

The experimental setup was described in detail elsewhere [1, 10, 11]. The ultrasound frequency was 22 kHz, the total absorbed ultrasonic power (40 W) was measured calorimetrically. The 0.26 nm resolution spectra of multibubble SL of argon saturated NaCl aqueous solutions were measured at a temperature range 5-15 ºC, concentration range 0.5-4 M and hydrostatic pressure range 1-2 bar. No significant changes of the form D-line Na in the range of experimental conditions were noted. To improve the signal to

noise ratio the spectra were summarized (Figure 2, curve 1). The spectrum of the flame with the addition of NaCl was measured at the same resolution of the spectrometer (Figure 2, curve 3).

DENSITY INSIDE A BUBBLE

Figure 1a shows the radius R and temperature T inside a bubble shortly before collapse for classical model [12], as well as the density n calculated from radius under an assumption that the time is not enough for mass transfer. According to [12], for SBSL and frequency of 26.5 kHz the bubble becomes heat- and mass- isolated system by a time of 20 ns before t=0. We can estimate peak density using Figure 1a. Let's suppose that for t=-20 ns the value of density in the bubble is still close to normal, n_a=1 Amg (1 Amg = $2.6868 \cdot 10^{19}$ cm^{-3}). The radius decreases from R_a~8 μm to R_{min}~0.8 μm at t=0. Then from $n_{peak}/n_a=(R_a/R_{min})^3$ we obtain n_{peak}=1000 Amg. Note that the density of water is about 1240 Amg under normal conditions. Hence, the peak density of intrabubble content can reach the density of a liquid.

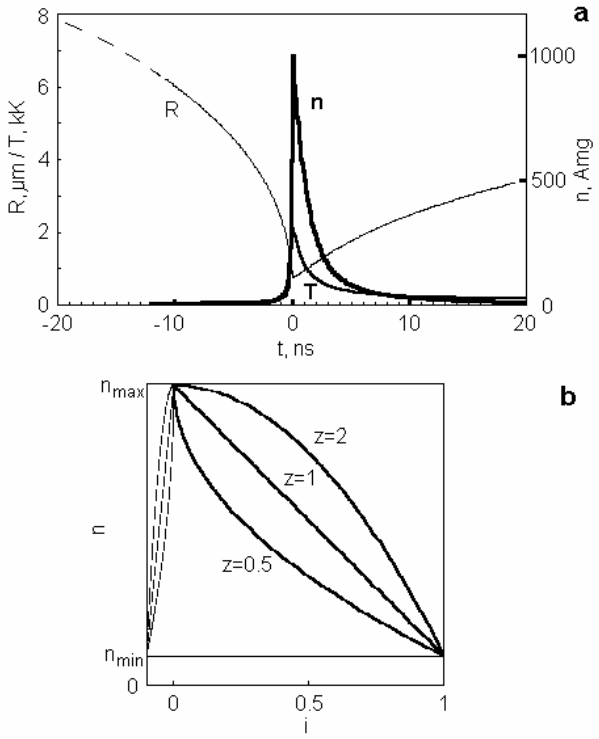

Figure 1. (a) Radius R, temperature T (reproduced from [12]) and density n dynamics of bubble driven at 26.5 kHz shortly before collapse; (b) three cases of model dynamics of density n; i - integration variable; z, n_{min}, n_{max} – model parameters.

Using the broadening coefficient [13], we get the width at the half-maximum of Na line about 20 nm for this density. In experimental spectra the value is about 3 nm. The lower peak density may be the reason. The other explanation is that the Na emission occurs far from the point t=0. As already mentioned, in [7] was measured that in the laser-created bubble the Na emission (585-595 nm) becomes apparent far from the collapse point (150 ns for low salt concentration). The D-line signal reaches a maximum and then decreases prior to the occurrence of the blackbody signal (250-450 nm). The effect is in agreement with calculations [9], according to which in SL spectra for 85% H_2SO_4 atomic and molecular lines are apparent in t=-2 ns, while the continuum is dominant in the moment of collapse and after it.

Narrow parent peaks of the Na doublet (<0.4 nm) in SL spectra [3, 6] cannot be radiated near the moment t = 0. As will be shown, within our model the well-resolved doublet appears in spectra at density less than 5 Amg (Figure 2, curves 3').

We assume that the spectrum is integrated, and an integration parameter is unambiguously linked to the density of environment. The time of emission can be such a parameter. This supposition has appeared sufficient for an explanation the Na D-line shape in SL, including the width, asymmetry, shift of the maximum and the presence of parent peaks. The fitting of the model spectra to experimental data has allowed making an estimation of the upper and lower thresholds of the densities of perturbing surrounding during the Na emission. In the calculations we use the review [13], where theoretical and experimental data of the modification of spectral lines by a density of other neutral particles are collected.

The interactive algorithm of the model is implemented within the Microsoft Excel. The results are demonstrated in Figures 2-5.

MODEL

According to [13], the shift and broadening of alkali metals spectral line profiles by foreign particles depend on density almost linearly:

$$\Lambda(n) = \Lambda_0+\sigma n, \qquad S(n) = S_0+\gamma n, \tag{1}$$

where $\Lambda(n)$ – wavelength of line maximum shifted at density n, S(n) – half-width of the line at density n, Λ_0 – initial wavelength (at low pressure), S_0 – initial half-width of the line, n – density, σ and γ - shift and broadening factors.

We approximate the line profile by two Gaussian curves because the doublet components are resolved. It is shown [13] that at very high density the line profile assumes a Gaussian character for any kind of model potential:

$$G(\lambda) = (C_1/S_1)\cdot\exp(-½(\Lambda_1-\lambda)^2/S_1^2) + \\ + (C_2/S_2)\cdot\exp(-½(\Lambda_2-\lambda)^2/S_2^2), \tag{2}$$

where λ – wavelength, C_1, C_2 – normalization factors, S_1, S_2 – half-width at half-maximum, Λ_1, Λ_2 – wavelengths of the doublet components. The values of S_1, S_2, Λ_1, Λ_2 depend on n (1). Taking n=0, we select the initial values of S_{01}, S_{02}, Λ_{01}, Λ_{02}, using the spectrum of flame as the initial spectrum for simulating a curve (2). Having substituted $\Lambda_j(n)$ and $S_j(n)$, where j=1,2 – the doublet components, in (2) and having set the density n in the range from 10 to 100 Amg with a step of 10 Amg, we receive the profile of Na line for each value of density (Figure 2, the set of lines 3').

The density curve during Na emission is a parameter. We set the function n(i) for model curve (Figure 1b):

$$n(i)=n_{max}\cdot(1-i^z)+n_{min}\cdot i^z, \tag{3}$$

where n_{max} and n_{min} – upper and lower values of the range when the Na emission occurs, z – density curve degree, $0 \le i \le 1$ – integration variable. Let's consider three cases (Figure 1b): z=0.5 – the density grows with acceleration, z=1 – linear growth, z=2 – growth with deceleration by the moment of i=0. These cases differ by the contribution of spectra of various densities to the total spectrum. Note that neither reversing of the direction along the axis i nor the rescaling along the axis i is not significant from the point of view of our model.

We calculate the total spectrum as:

$$H(\lambda) = K\cdot\int_0^1 G(\lambda,n(i))di, \quad (4)$$

where K – normalization factor at 589 nm. The asymmetry of total spectrum arises due to the integration of spectra with different width which are regularly shifted from each other.

For the explanation of the intensity of parent peaks we introduce one more parameter d - an additional fraction of "low density" spectrum. The final equation is

$$H(\lambda) = K\cdot(d\cdot G(\lambda,0)+(1-d)\int_0^1 G(\lambda,n(i))di). \quad (5)$$

Let us note some details of the model. The shift, width and asymmetry of atomic lines depend on many parameters. We consider here the density of perturbing particles is the main reason of the Na line distortion. We believe the bubble is optically transparent. If the bubble is opaque, the contribution of the Na emission to total spectrum will be suppressed. We believe that the amount of emitting atoms remains constant, and the oscillator strength of the Na D-line does not vary. Note that some of these effects can be included implicitly in n(i). The instrumental line width is included in constant S_0 (1).

According to [14], the bubble consists of 14% water and 86% argon. According to [13], the shift σ and half-width γ of the Na D-line by Ar for the first doublet component $3s^2S_{1/2} \rightarrow 3p^2P_{3/2}$ (589 nm) are σ_1=-7.5·10^{-21} cm^{-1}/cm^{-3} and γ_1=1.17·10^{-20} cm^{-1}/cm^{-3}, accordingly; and for the second component $3s^2S_{1/2} \rightarrow 3p^2P_{1/2}$ (589.6 nm) σ_2=-6.8·10^{-21} cm^{-1}/cm^{-3} and γ_2=1.41·10^{-20} cm^{-1}/cm^{-3}, accordingly. We enumerate cm^{-1}/cm^{-3} on nm/amg for σ and γ (Table 1). Because of the small spectral range we neglect mutual nonlinearity of scales of nanometer and cm^{-1}.

The values are determined for temperatures of 400÷600 K, while the multibubble "cavitation temperatures" are about 2000÷5000 K. In [13] the most of the data is given for a density having an order of 10^{20} cm^{-3} whereas in the collapsing bubble the order of density can exceed 10^{22} cm^{-3}. In addition, there are other particles inside the cavitation bubble. In [3] the broadening of Na line by argon γ=3.31·10^{-20} cm^{-1}/cm^{-3} (for T~2000 K) exceeds the factor, given in [13], in 2.5 times.

So n_{min}, n_{max}, z and d are the parameters of the model. The line shift and broadening factors can be the parameters too. Within our model doubled value of σ compared to [13] gives the best correspondence to experimental data (Table 1).

Table 1. The Na line shift σ and half-width γ by Ar

j	λ, nm	σ, nm/Amg	*σ', nm/Amg	γ, nm/Amg
1	589	0.0070	0.0140	0.0109
2	589.6	0.0064	0.0128	0.0131

*σ' – the σ values which we use in the model

The results of calculations H(λ) (5), thin lines 1a', 1b', 1c', 2', and experimental spectra, thick lines 1 and 2 (the spectrum 2 is taken from [4]) are shown in Figure 2. We can see the case z=0.5 gives the best agreement with experimental data. The inset in Figure 2 shows one more SL spectrum of Na with parent peaks [6] and its model.

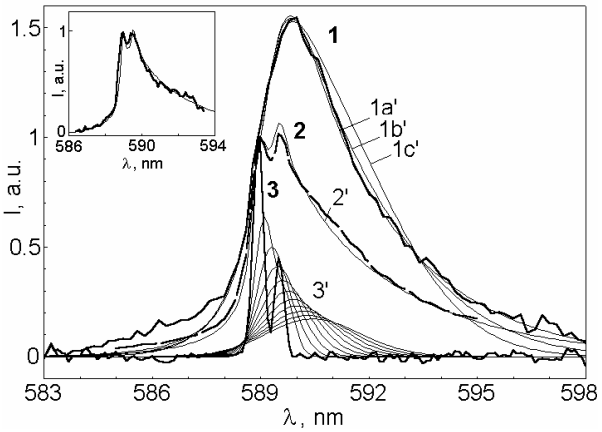

Figure 2. Experimental and model spectra of Na D-line. Thick line 1 - SL spectrum NaCl aqueous solution at 22 kHz, 0.26 nm resolution; thick line 2 - SL spectrum of NaCl solution at 138 kHz, 0.315 nm resolution (reproduced from [3]); thick line 3 - flame spectrum of NaCl, 0.26 nm resolution. Level of a continuum for experimental spectra is taken as zero. Thin lines 1a', 1b', 1c' - models of spectrum 1 with parameters: z=0.5, 1, 2, n_{max}=420, 250, 180 Amg, n_{min}=28, 26, 23 Amg, accordingly; d=0. Thin line 2' - model of spectrum 2 with parameters z=0.5, n_{max}=500 Amg, n_{min}=10 Amg, d=0.05. All spectra are normalized at 589 nanometers. Set of thin curves 3' - model spectra, calculated in density range of 10-100 Amg with a step of 10 Amg, square normalized. The inset shows SL spectrum at 460 kHz, 0.2 nm resolution (reproduced from [6]) and its model with parameters z=0.5, n_{max}=600 Amg, n_{min}=6 Amg, d=0.03.

PERFORMANCE OF MODEL

The simulation of experimental spectra by model spectra is successful. The "low density" emission imports the contribution to the part near to the parent peaks whereas the "high density" emission increments intensity of the spectra far and to the right of the doublet. Let's consider the sensitivity of the model to variation of its parameters. The increase of σ/γ ratio leads to the change of the declination of a model spectrum at 589 nm, as well as spectrum intensity at the left and right wings far away the maximum. In a case n_{max} increases, the long-wave wing of the line becomes higher. The increase of z leads to the broadening of the line profile. In order to avoid this it is necessary to decrease n_{max} simultaneously with the increase of z. However, this leads to the change of the declination of model spectrum to the right of the maximum (Figure 2, lines 1a', 1b', 1c'). We can see that the case z=0.5 is the most successful. This means that during Na emission the growth of the density accelerates towards the point i=0 (Figure 1b). In a case if Na emission occur near to the point of full collapse, the variant z=2 would be in favor. The increase of n_{min} leads to appreciable growth of intensity of the line to the right of 589 nm and, simultaneously, to the shift of maximum. In order to compensate this we should decrease n_{max} that leads to the change of the declination of model spectrum to the right of the maximum, and its shape becomes more symmetric. The decrease of n_{min} (n_{min}<10 Amg) yields the same effect, as the increase of d. The contribution of the "low density" spectra of d~3-5 % to the sum spectrum is enough for justifying the Na parent peaks.

Let's consider one more case when the density is set by curve n(t) (Figure 1a), and parameter z is absent, Figure 3a. However, the line shape is simulated not so well than in the case when the curve n(i) is chosen (Figure 1a). It seems n(i) is more suitable for describing the density change during the Na emission. For this case of the model, there is a big range

of n_{max} (at $n_{max} >> n_{min}$) when the model line shape does not vary noticeably. This results from the fact that, for fixed n_{min}, the increase of n_{max} leads to the increase of the contribution of spectra for densities, comparable with n_{min} and no so much to the growth of the contribution of spectra of high densities. From the point of view of mathematics it means that there should be such kind of dependence n(i) at which the parameter n_{max} can be excluded from the model.

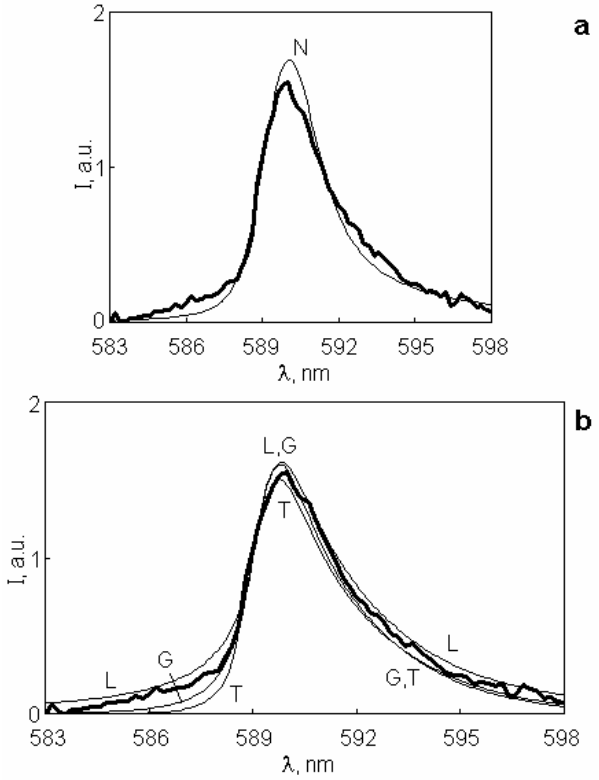

Figure 3. Different models of spectrum 1 from Figure 2 (thick line): (a) thin line N – density is set by curve n(t) (Figure 1a) with parameters n_{max}=1000 Amg, n_{min}=50 Amg, d=0; (b) thin lines L, G, T – for Lorentz, Gauss, triangular approximations (2), accordingly, with parameters n_{max}=400 Amg, n_{min}=25 Amg, d=0, z=0.5.

The function n(i) can be restored from an experimental spectrum. For this purpose the experimental curve should be measured very precisely.

For the purpose to show how the kind of approximation (2) affects the integral spectrum we compare the Gauss, Lorentz and triangular approximations of initial line (Figure 3b). It is obvious that the kind of approximation is insignificant. The using of Lorentz curve gives a little better result in the short-wave region.

DISCUSSION

The magnitude of the half-width at half-maximum of the Na line, taking into account the instrumental slit half-width, and the shift of the middle of the line, allows to estimate the density: by broadening 106 and 88 Amg, and by shift 94 and 61 Amg, for spectra 1 and 2 on Figure 2, accordingly. The values proposed in [11, 3] are 70 and 60 Amg, accordingly. Certainly, these estimations give the values of some average density during the emission time. We can estimate the pressure from P=nkT. Using T~2000 K and n_{max}=400 Amg, we get P_{max}~3000 bar for the spectrum 1 (Figure 2). This value is higher than the estimation of peak pressure given by us in [11].

Let's notice that the accuracy of the estimations directly depends on factors σ and γ, which precisely are not defined for two reasons: high values of density for which factors are not studied, and presence of others (in addition to argon) perturbing particles. If we assume Na emits from a liquid/bubble boundary layer [1] water will be the basic perturbing substance. It can be a possible explanation of the independence of width and shift of SL line from the type of saturating gas [5], and also of other, in comparison to argon, σ /γ.

MODELLING OF K AND LI LINES

Figure 4 reproduces the SL spectra for KCl in water at different ultrasound frequencies (from [15]) (a), and the model spectra (b). The model parameters are specified in the captions. For calculations the line shift was increased by a factor of 1.5 concerning [13] for potassium in argon. The simulation shows that the decrease of ultrasound frequency from 1000 to 28 kHz leads to the increase of n_{max} from 150 to 550 Amg, the increase of n_{min} from 0 to 25 Amg and to the decrease of d from 0.3 to 0.02. The higher values of n_{max} are achieved at the lower ultrasound frequencies. The dependence on the ultrasound frequency [15] can be related to a smaller size of cavitation bubbles formed at higher frequencies and, hence, different conditions during the collapse.

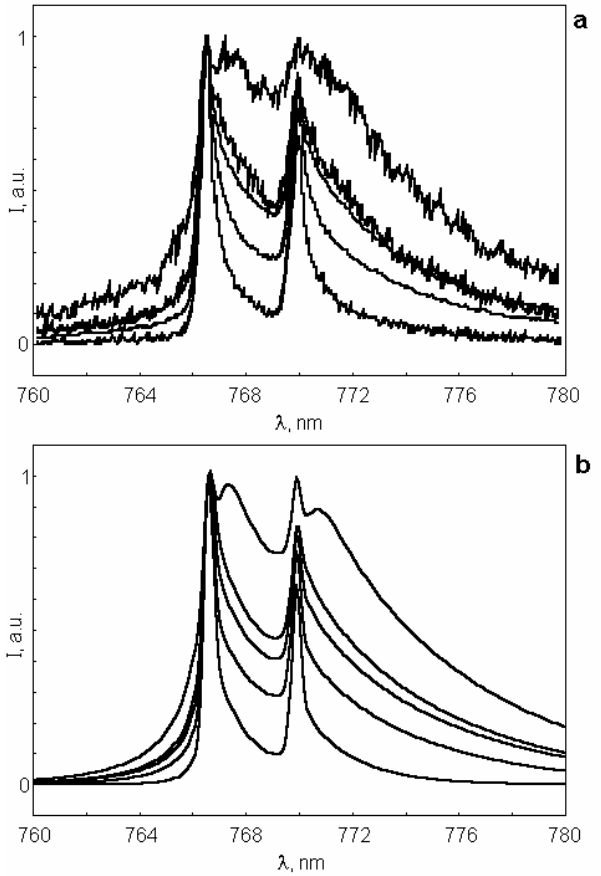

Figure 4. (a) SL spectra (reproduced from [15]) of K from KCl aqueous solution saturated with Ar at ultrasound frequency: 1MHz, 510, 115, 48, 28 kHz. (b) Models of K line with parameters: n_{max}=150, 400, 500, 500, 550 Amg; n_{min}=0, 0, 0, 4, 25 Amg; d=0.3, 0.08, 0.03, 0.03, 0.02, accordingly; z=0.5. From the bottom to the top of the figure.

Figure 5 reproduces the SL spectrum for LiCl in water in comparison with the spectrum of flame and the spectrum calculated within our model. The shift σ increased doubly concerning [13] for Li in Ar was used for the calculation.

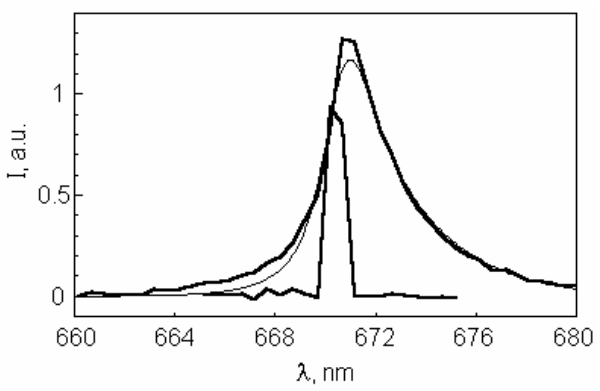

Figure 5. Thick lines - SL spectrum of LiCl aqueous solution in Ar at 20 kHz and flame fluorescence spectrum of LiCl, 0.65 nm resolution; thin line - model with parameters n_{max}=360 Amg; n_{min}=20 Amg; d=0, z=0.5.

CONCLUSION

We present the simple model for a Na D-line in sonoluminescence based on suppose that the line profile is formed by contributions of spectra from luminescent areas with different density during the emission time. Using the model the lower and the upper values of density in the cavitation bubbles, when Na emission occurs, were estimated. Comparing the calculated and observed spectra we conclude the better agreement is for the case when the density rate is accelerates to the moment of full collapse. We also propose that the only origin of parent unshifted Na D-line doublet peaks observed in the experimental spectra is "low density" emission.

REFERENCES

1 T.V. Gordeychuk, M.V. Kazachek, "Experimental observation of the intense enhancement of metal sonoluminescence under pressure and temperature" *Optics and Spectroscopy* **106**, 238-241 (2009)

2 F. Lepoint-Mullie, N. Voglet, T. Lepoint, R. Avdi, "Evidence for the emission of 'alkali-metal – noble-gas' van der Waals molecules from cavitation bubbles" *Ultrason. Sonochem.* **8,** 151-158 (2001)

3 P.K. Choi, S. Abe, Y. Hayashi, "Sonoluminescence of Na atom from NaCl solutions doped with etanol" *J. Phys. Chem. B* **112,** 918-922 (2008)

4 D.J. Flannigan, S.D. Hopkins, C.G. Camara et.al. "Measurement of Pressure and Density inside a Single Sonoluminescing Bubble" *Phys. Rev. Lett.* **96,** 204301(4) (2006)

5 E.B. Flint, K.S. Suslick, "Sonoluminescence from Alkali-Metal Salt Solutions" *J. Phys. Chem.* **95,** 1484-1488 (1991)

6 C. Sehgal, R.P. Steer, R.G. Sutherland, R.E. Verrall, "Sonoluminescence of argon saturated alkali metal salt solutions as a probe of acoustic cavitation" *J. Chem. Phys.* **70,** 2242-2248 (1979)

7 H.C. Chu, S. Vo, G.A. Williams, "Precursor Luminescence near the Collapse of Laser-Induced Bubbles in Alkali-Salt Solutions" *Phys. Rev. Lett.* **102**, 204301(4) (2009)

8 B. Gompf, R. Gunther, G. Nick et al., "Resolving sonoluminescence pulse width with time-correlated single photon counting" *Phys. Rev. Lett.* **79,** 1405-1408 (1997)

9 Yu An, C. Li, "Diagnosing temperature change inside sonoluminescing bubbles by calculating line spectra" *Phys. Rev. E* **80,** 046320(6) (2009)

10 Y.T. Didenko, T.V. Gordeychuk, V.L. Korets, "The effect of ultrasound power on water sonoluminescence" *J. Sound. Vibr.* **147,** 409-416 (1991)

11 M.V. Kazachek, T.V. Gordeychuk, "Estimation of the Cavitation Peak Pressure Using the Na D-line Structure in the Sonoluminescence Spectra" *Tech. Phys. Lett.* **35,** 193-196 (2009)

12 M.P. Brenner, S. Hilgenfeldt, D. Lohse, "Single-bubble sonoluminescence" *Rev. Mod. Phys.* **74,** 425-484 (2002)

13 N. Allard, J. Kielkopf, "The effect of neutral nonresonant collitions on atomic spectral lines" *Rev. Mod. Phys.* **54,** 1103-1181 (1982)

14 B.D. Storey, A.J. Szeri, "Water vapour, sonoluminescence and sonochemistry" *Proc. R. Soc. London. Ser. A.* **456,** p. 1685-1709 (2000)

15 Sh. Abe, P.-K. Choi, "Effect of Frequency on Sonoluminescence Spectrum from Alkali-Metal Solutions" *Nonlinear Acoustics—Fundamentals and Applications (ISNA 18)* CP1022, 189-192 (2008)